CHARACTERISATION OF COMPONENTS OF A SCINTILLATION-FIBER-BASED COMPTON CAMERA*

A. Wrońska[a,†], R. Hetzel[b], J. Kasper[b], R. Lalik[a]
A. Magiera[a], K. Rusiecka[a], A. Stahl[b]

[a]M. Smoluchowski Institute of Physics, Jagiellonian University, Kraków, Poland
[b]Physics Institute III B, RWTH Aachen University, Aachen, Germany

The next awaited breakthrough in proton therapy is the inclusion of the tools for online monitoring of beam range into clinical practice. Full, three-dimensional information on the deposited dose distribution can be obtained by means of prompt gamma imaging using Compton cameras. Large gamma detection efficiency and high-rate capacity can be achieved using detectors of high granularity made of a heavy scintillator. One of the possible design options is a stack of scintillating fibers. As the overall performance of such a camera depends on the position, time and energy resolution of the fibers, we investigate those properties both experimentally in measurements with a test bench as well as via Monte Carlo simulations. The obtained results point at LYSO:Ce as the best candidate for a sensitive material of a Compton camera of the discussed type.

1. Introduction

Particle therapy has become a very popular treatment modality of tumours thanks to a favourable dose depth profile compared to conventional radiotherapy. However, over the last decade, an opinion has been established in the community that the next steps to fully utilize the potential of proton therapy should be to develop methods for its online monitoring [1]. The quantity which should be verified in the course of the therapy is proton beam range or — in a differential approach — spatial distribution of the dose deposited in the course of the therapy. One of the possible ways

---

† Corresponding author: aleksandra.wronska@uj.edu.pl

to achieve it is based on registration of prompt gamma (PG) radiation, a by-product of beam interaction with the patient's tissue. An overview of different approaches to the problem can be found in [2].

2. Rationale for a fiber-based design of a Compton camera

Among the methods exploiting PG, most advanced in R&D are those requiring simple detection techniques and delivering information on beam range, such as a slit-camera [3] or a spectroscopic setup described in Ref. [4]. To investigate the spatial distribution of a delivered dose, one needs a Compton camera (CC), capable of delivering a three-dimensional image. The working principle of a CC requires registration of a position and energy of each detected PG quantum in two modules of the detector. The position and energy resolution, together with collected statistics, define the resolution of the reconstructed image. The latter seems to be a limiting factor for setups based on semiconducting detectors. Therefore, the interest has been directed towards detectors based on heavy scintillators [5–7]. In this work, we present activities towards a development of a CC consisting of fibers made from such a material. The design ensures, apart from large detection efficiency, also high count rate capacity, and the position resolution can be tuned by fiber dimensions. Moreover, some modern materials exhibit also excellent timing resolution, allowing to impose tight cuts on coincidences between hits in two modules, which reduces background from accidental coincidences. In this work, we present the investigation of properties of fibers made from various materials along with the algorithms for position and energy reconstruction developed using Geant4 simulations.

3. Experimental survey of available materials

While designing a detector for medical imaging purposes, a number of requirements for the scintillating material has to be considered in order to provide the best performance of the device [8]. In the case of the proposed detection setup, those requirements include: a large density and Z_{eff}, an emission spectrum compatible with available SiPMs spectral range and a short decay constant, which is important from the point of view of rate capacity of the detector. Also large light yield is desired, since it directly influences the energy and position resolution. Moreover, excellent energy resolution is required for precise determination of the Compton scattering angle in the image reconstruction process. The selected scintillating material should also be transparent for its own scintillating light, so the correlated signals stemming from the same interaction can be registered at both ends of the fiber. On the other hand, the position resolution is proportional to the attenuation length, thus large attenuation lengths are not desired. A rea-

sonable compromise is 10–20 cm. Many available scintillating materials are radioactive themselves due to content of heavy elements or doping with rare earth elements. Intrinsic activity of the scintillator is a source of additional accidental coincidences and background, which affects reconstructed image quality. Thus, scintillating material of low or none intrinsic activity is preferred. Additionally, the mechanical properties of the material should allow for machining in the desired elongated shape. Finally, price and availability have to be taken into account.

Based on those criteria, the following scintillating materials have been chosen for further investigation: LYSO:Ce, LuAG:Ce and GAGG:Ce[1]. In order to examine their properties, a dedicated test bench featuring an electronic collimation system has been built based on the design of Ref. [9]. The investigated fiber was coupled at both ends to Hamamatsu SiPMs (S13360-3050VE) with the use of Saint Gobain silicone gel and the signal wave forms were recorded using a CAEN Desktop Digitizer DT5742. For each fiber, a series of position-dependent measurements with an Na-22 radioactive source was recorded. All of the investigated samples had an elongated shape of the dimensions: $1 \times 1 \times 100$ mm^3. In the following part of this section, the investigated properties of the scintillators are described along with results obtained for the LYSO:Ce material that turned out to be best for the proposed detector design [10].

Assuming a simple model for the attenuation of the optical photons in the fiber, the deposited energy and the position of the interaction can be reconstructed by using only the number of recorded photons from the SiPMs at two ends of the fiber. The model assumes that the attenuation of the optical photons can be described by an attenuation factor caused by the material λ_{att} and an attenuation factor caused by the geometry of the fiber λ_{geo}. The signals recorded by the two SiPMs (S_1, S_2) are described by Eqs. (1), (2)

$$S_1(y) = S_0 \, \mathrm{e}^{-y/\lambda_{\mathrm{att}}} \, f(\lambda_{\mathrm{geo}}(y), y) \tag{1}$$

and

$$S_2(y) = S_0 \, \mathrm{e}^{-(L-y)/\lambda_{\mathrm{att}}} \, f(\lambda_{\mathrm{geo}}(L-y), L-y) \,, \tag{2}$$

where y is the position of the interaction along the fiber and L is its length. The ratio of correlated signals registered at both ends of the fiber allows to estimate light losses occurring during light propagation along the fiber using the quantity

$$M_{\mathrm{LR}}(y) = \ln\left(\sqrt{\frac{S_1(y)}{S_2(y)}} \right) = a_0 + \frac{y}{\lambda_{\mathrm{att}}} \,. \tag{3}$$

---

[1] Producers of the used scintillating fibers: LYSO:Ce — MetaLaser, LuAG:Ce — Crytur, GAGG:Ce — Fomos Materials.

Having a series of position-dependent measurements and associated M_{LR} distributions, one can determine the attenuation length λ_{att} by fitting Eq. (3) to the experimental points [11], as shown in Fig. 1. Light attenuation values for investigated fiber samples are the following: $\lambda_{\mathrm{att,LYSO:Ce}} = 165$ mm, $\lambda_{\mathrm{att,GAGG:Ce}} = 204$ mm, and $\lambda_{\mathrm{att,LuAG:Ce}} = 204$ mm.

The light output of the scintillating fiber is calculated as follows:

$$\mathrm{LO} = \frac{n_{\mathrm{PE}}\,(1 - f_{\mathrm{CT}})}{E\,C_{\mathrm{PDE}}\,\mathrm{e}^{y/\lambda_{\mathrm{att}}}} \qquad (4)$$

where n_{PE} is a number of photoelectrons corresponding to the $E = 511$ keV peak, f_{CT} is crosstalk probability and C_{PDE} is photodetection efficiency. It needs to be noted that the formula does not account for the losses due to fiber-SiPM coupling and geometry-specific effects (λ_{geo}). An example of summed light yield from both ends of the LYSO:Ce fiber as a function of the source position is shown in Fig. 1. For comparison, light output of GAGG:Ce is $\sim 93\%$ of LYSO:Ce and light output of LuAG:Ce is $\sim 43\%$ of LYSO:Ce.
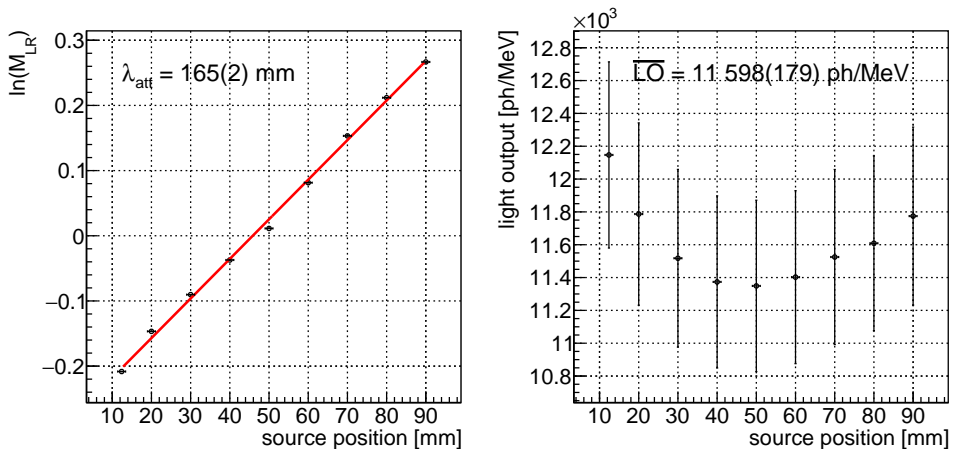

Fig. 1. Left: attenuation curve for LYSO:Ce fiber along with the fitted function given by Eq. (3). Right: dependence of summed light yield on radioactive source position for a LYSO:Ce fiber. Averaged light output $\overline{\mathrm{LO}}$ for this series is given. Error bars include contribution stemming from the energy resolution.

In order to determine the energy resolution σ_E/E, charge spectra from both ends of the investigated fiber, summed and corrected for light attenuation, have been used. The energy resolutions for the investigated materials determined for the 511 keV peak are as follows: $\sim 6.6\%$ for LYSO:Ce, $\sim 6.5\%$ for GAGG:Ce and $\sim 8.1\%$ for LuAG:Ce. Energy resolution of scintillating fibers is almost position-independent.

The decay constants of the investigated scintillators are determined by fitting a decay function to the falling slope of the registered signals (Fig. 2). In order to reduce the influence of statistical fluctuations, signals are averaged taking into account their amplitude and the time T_0, when the registered voltage reaches a set threshold. LYSO:Ce is characterized by a single decay process, thus the decay function can be presented as follows:

$$f(t) = A \, e^{-(t-t_0)/\tau} + \mathrm{BL} \,, \tag{5}$$

where A denotes the amplitude, t_0 is a time offset connected with the time when the signal reaches its maximal amplitude, τ is the decay constant and BL is the base line level. It needs to be noted that the used experimental technique and analysis methods allow to determine an effective decay constant, which results from the properties of both scintillating material and front-end electronics. The timing capacity of the proposed detection setup will in the end depend on the used scintillating material as well as electronic components, therefore, it is essential to determine such effective decay constants. The decay constant of the LYSO:Ce material determined as described above is $\tau \approx 64$ ns. In contrast to LYSO:Ce, GAGG:Ce and LuAG:Ce are characterized by a double decay process. Decay constants of GAGG:Ce are $\tau_{\mathrm{fast}} \approx 100$ ns ($\sim 80\%$) and $\tau_{\mathrm{slow}} \approx 450$ ns ($\sim 20\%$). For LuAG:Ce $\tau_{\mathrm{fast}} \approx 140$ ns ($\sim 30\%$) and τ_{slow} exceeds 1 μs[2].
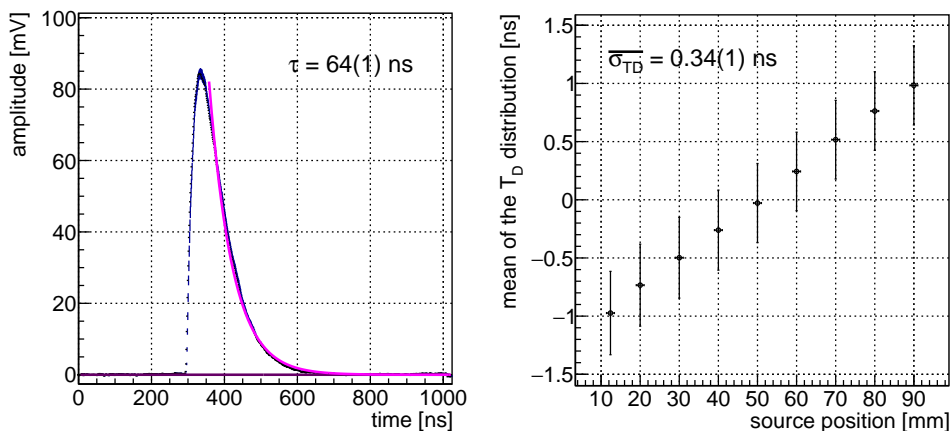

Fig. 2. Left: averaged signal registered from LYSO:Ce fiber along with the fitted decay function. Right: dependence of the mean T_D on the radioactive source position. Vertical error bars represent time resolution. Average time resolution $\overline{\sigma}_{T_D}$ calculated for the series is given.

[2] The applied acquisition window of 1 μs was insufficient to determine the long decay constant τ_{slow} with a better accuracy.

The time resolution is determined by analysing the time differences between correlated signals registered at both ends of the fiber $T_D = T_{0,ch0} - T_{0,ch1}$. Figure 2 shows a dependence of the mean T_D on the source position for a LYSO:Ce fiber. Vertical error bars correspond to the time resolution. In order to eliminate the walk effect, only events forming the 511 keV peak have been included. Obtained timing resolution for LYSO:Ce fiber is $\overline{\sigma}_{T_D} = 0.34$ ns. For comparison, the timing resolutions of GAGG:Ce and LuAG:Ce are 0.48 ns and 2.1 ns, respectively.

4. Geant4 simulations of fiber performance

A single fiber, coupled to two SiPMs at the ends, is simulated in Geant4 with the purpose to determine resolutions as functions of gamma energy. Additionally, the results of these simulations are used to develop a method to reconstruct the deposited energy and the position of the interaction along the fiber.

The simulated setup is shown in Fig. 3 on the left side. The simulation contains a LYSO:Ce-fiber, which performed best in the laboratory tests, of the size $1 \times 1 \times 100$ mm^3. While in Section 3 the results for a naked fiber are presented, in the simulations the fiber is coated with a dispersive titanium paint of a thickness of 0.01 mm and coupled to two 1 mm^2 SiPMs via a 0.1 mm thick layer of optical gel. The used Geant4 version is 10.04.p02 and in addition to the predefined physics list QGSP_BIC_HP_EMZ, the simulation of optical photons is activated. The number of simulated optical photons counted by an SiPM is adjusted taking into consideration a model of an SiPM describing its PDE, dark noise and cross talk.
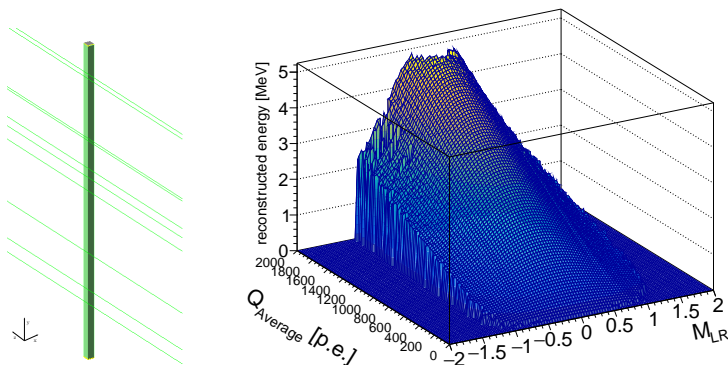

Fig. 3. Left: sketch of the simulated setup. The LYSO:Ce fiber is coated with a titanium paint and coupled via an optical gel to the SiPMs. The direction of the simulated primary photons is also shown. Right: look-up table for the deposited energy.

Equations (1), (2) show that $Q_{\text{Average}} = \sqrt{S_1 S_2}$ is proportional to the number of scintillation photons produced in the fiber S_0 and thus to the deposited energy E_{dep}. The variable M_{LR} introduced before is proportional to the position of the interaction along the fiber. Based on these two variables, look-up tables (LUTs) to reconstruct the energy and position of the interaction are constructed. To take into account the influence of $f(\lambda_{\text{geo}}(y), y)$, the tables are built depending on both variables. To build the LUTs, the interactions of photons with energies from 0.5 MeV to 6 MeV are simulated all along the fiber. For each interaction, M_{LR} and Q_{Average} are calculated and sorted into bins. For each resulting M_{LR} and Q_{Average} pair, the distributions of the energy and position are fitted with a Gaussian function to determine the most probable values for the reconstruction. For the uncertainty of a reconstructed value, two more LUTs are built, which are filled with the standard deviations resulting from the fits instead of mean values. The resulting LUT for the energy reconstruction is shown in Fig. 3.

These LUTs are used to perform reconstruction of position and energy deposits on a different set of simulated events. The differences of the simulated and reconstructed positions and energies are given in Figs. 4 and 5. The resulting resolutions are shown as well.
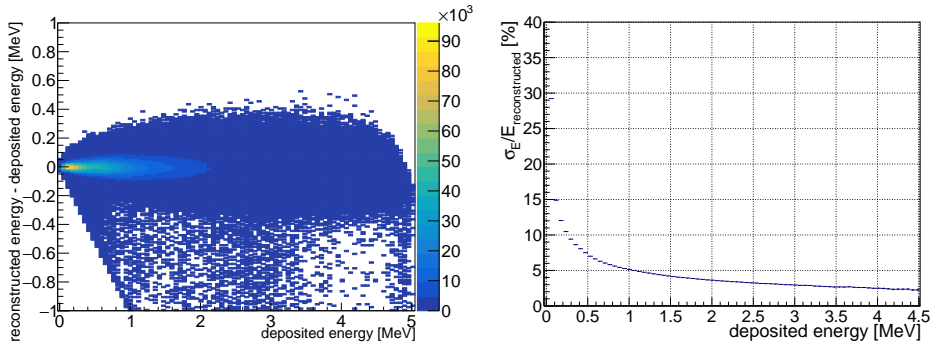

Fig. 4. Left: difference between the reconstructed and simulated energies plotted *versus* the simulated energy. Right: resulting resolution of the energy reconstruction via LUTs.

The LUTs yield to an energy resolution of $\sim 7\%$ at 511 keV, which improves for higher energies to $\sim 3\%$. The position resolution is strongly dependent on the position along the fiber. In the middle of the fiber, a resolution of about 6.5 mm is reached which improves towards the ends to about 0.5 mm. This effect is caused by photons that are not reflected at the surface of the fiber but reach directly the SiPMs. Closer to the fiber ends the number of these photons drastically increases which yields to the improved resolution. The position resolution averaged over the fiber improves by a factor of ~ 2.5 from the energy of 511 keV to 4.4 MeV.
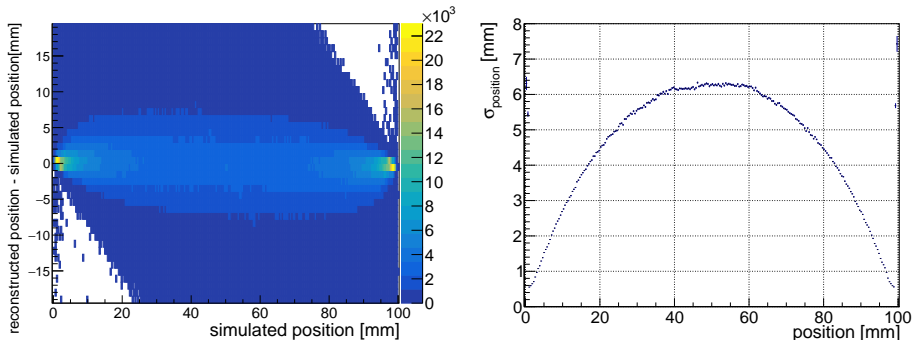
Fig. 5. Left: difference between the reconstructed and simulated positions plotted against the simulated position. Right: resolution of the LUT method of position reconstruction.

5. Conclusions

We have conducted a series of real and virtual experiments aiming at the determination of scintillating fiber properties. The dimensions of the investigated fibers were $1 \times 1 \times 100$ mm^3. Among the three tested materials: LuAG:Ce, LYSO:Ce and GAGG:Ce, LYSO shows the best performance in terms of light output, and is comparable or better in terms of energy and time resolution and signal duration. It is also widely available and inexpensive, compared with other materials. The drawback of intrinsic radioactivity turns out negligible when building coincident events from hits in the two detector modules. The simulated and measured energy resolution agree at 511 keV and yield 6–7%. The simulations indicate, that at higher energies a resolution as good as 3% can be expected. Position resolution along the fiber found in the simulations is about 6 mm near the fiber center and < 1 mm close to the ends. This is insufficient for a CC, therefore, other methods allowing to improve it are investigated. One of the possible solutions is a setup geometry in which the neighbouring layers have different fiber orientation. This option is currently under study.

REFERENCES

[1] NuPECC report 2014: Nuclear Physics for Medicine,
   `http://www.nupecc.org/pub/npmed2014.pdf`

[2] J. Krimmer *et al.*, *Nucl. Instrum. Methods Phys. Res. A* **878**, 58 (2018).

[3] Ch. Richter *et al.*, *Radiother. Oncol.* **118**, 232 (2016).

[4] F. Hueso-González *et al.*, *Phys. Med. Biol.* **63**, 185019 (2018).

[5] A. Koide *et al.*, *Sci. Rep.* **8**, 8116 (2018).

[6] P. Bennati *et al.*, *JINST* **12**, C05009 (2017).

[7] K. Shimazoe *et al.*, *Nucl. Instrum. Methods Phys. Res. A* (2018),
   DOI:10.1016/j.nima.2018.10.177.

[8] P. Lecoq, *Nucl. Instrum. Methods Phys. Res. A* **809**, 130 (2016).

[9] P. Anfré *et al.*, *IEEE Trans. Nucl. Sci.* **54**, 391 (2007).

[10] K. Rusiecka *et al.*, in: Engineering of Scintillation Materials and Radiation
   Technologies Selected Articles of ISMART2018, (Eds.) M. Korzhik,
   A. Gektin, Springer, 2019, p. 195.

[11] K. Pauwels *et al.*, *JINST* **8**, P09019 (2013).